Theoretical spectroscopic parameters for isotopic variants of HCO + and HOC +

Mirjana Mladenović

▶ **To cite this version:**

HAL Id: hal-01599204
https://auf.hal.science/hal-01599204

Submitted on 4 Oct 2017

Theoretical spectroscopic parameters for isotopic variants of HCO$^+$ and HOC$^+$

Mirjana Mladenović*

Université Paris-Est, Laboratoire Modélisation et Simulation Multi-Echelle (MSME),
UMR 8208 CNRS, 5 bd Descartes, 77454 Marne la Vallée, France

Theoretical spectroscopic parameters are derived for all isotopologues of HCO$^+$ and HOC$^+$ involving H, D, ^{16}O, ^{17}O, ^{18}O, ^{12}C, and ^{13}C by means of a two-step procedure. Full-dimensional rovibrational calculations are first carried out to obtain numerically exact rovibrational energies for $J = 0 - 15$ in both parities. Effective spectroscopic constants for the vibrational ground state, ν_1, ν_2, and ν_3 are determined by fitting the calculated rovibrational energies to appropriate spectroscopic Hamiltonians. Combining our vibration-rotation corrections with the available experimental ground-state rotational constants, we also derive the new estimate for the equilibrium structure of HCO$^+$, r_e(CH)=1.091 98 Å and r_e(CO)=1.105 62 Å, and for the equilibrium structure of HOC$^+$, r_e(HO)=0.990 48 Å and r_e(CO)=1.154 47 Å. Regarding the spectroscopic parameters, our estimates are in excellent agreement with available experimental results for the isotopic variants of both HCO$^+$ and HOC$^+$: the agreement for the rotational constants B_v is within 3 MHz, for the quartic centrifugal distortion constants D_v within 1 kHz, and for the effective ℓ-doubling constants q_v within 2 MHz. We thus expect that our results can provide useful assistance in analyzing expected observations of the rare isotopologues of HCO$^+$ and HOC$^+$ that are not yet experimentally known.

I. INTRODUCTION

Electrons and ions play a significant role in interstellar physical chemistry and for the modelling of the composition of the interstellar medium. Knowledge about their abundances gives important information regarding the sources which heat and ionize the gas. Protonated carbon monoxide may appear as the formyl cation, HCO$^+$, or as the isoformyl cation, COH$^+$. The formyl cation is an abundant species in outer space, observable in many objects. In ion-molecule chemistry, HCO$^+$ is the cornerstone species with an important role in astrochemical models of chain reactions leading to the formation of organic molecules.[1] The formation and depletion mechanism of HOC$^+$, as well as the abundance ratio [HCO$^+$]/[HOC$^+$], have attracted a lot of interest.[2,3] HCO$^+$ and HOC$^+$ remain the only known example of isomeric interstellar ions.[4,5]

During a search for HCN, Buhl and Snyder detected a new molecular line at 89.190 GHz in several interstellar media, whose carrier was named X-ogen, meaning that "it has an extraterrestial origin".[6] The assignment of this transition to HCO$^+$ proposed by Klemperer[7] was confirmed in the laboratory by Woods and coworkers[8] five years later. Since then the rotational spectrum of HCO$^+$ has been extensively studied.[1,9–13] The recording of the pure rotational transitions in the ground vibrational state has been extended up to 1.6 THz, i.e. the transition $J = 17 \to 16$.[13] The band origins for all three vibrational fundamentals were determined by infrared laser spectroscopy, covering the stretching ν_1 mode,[14,15] the bending ν_2 mode,[16,17] and the stretching ν_3 mode.[18,19] The hot bands in the region of ν_1 and ν_3 are also known.[20–22] Some higher vibrationally excited states of HCO$^+$ were characterized experimentally.[23–25] Rotational transitions in the vibrationally excited state could be of astronomical interest in hot, dense environments. The stability of HCO$^+$ is apparent from the low ionization potential of HCO of 8.27 eV known from photoelectron spectroscopy.[26] In outer space, HCO$^+$ has been detected in various regions, such as e.g. star-forming regions,[27,28] diffuse clouds,[29] circumstellar envelopes,[30] and circumstellar disks.[31,32]

The first spectroscopic detection of HOC$^+$ was made in 1982 by Gudeman and coworkers,[33,34] who observed the lowest ($J = 0 \to 1$) rotational transition of HOC$^+$, HO^{13}C$^+$, and H^{18}OC$^+$ in laboratory direct-current glow discharges. Blake at al.[35] extended the laboratory measurements up to 350 GHz by recording the rotational transitions up to $J = 3 \to 4$. Woods et al.[36] undertook a detailed search in the interstellar medium at 14 different locations, tentatively identifying a weak emission line in Sgr B2 as the $J = 1 \to 0$ transition of HOC$^+$. This detection was, however, viewed with skepticism because of the high reactivity of HOC$^+$. The observation reported by Ziurys and Apponi[37] towards several sources provided a final confirmation of interstellar HOC$^+$. Since then HOC$^+$ has been observed in interstellar environments in both dense[36–38] and diffuse[39] molecular clouds, including photon-dominated regions.[40] Isomer ratios [HCO$^+$/HOC$^+$] between 300 and 6000 are reported in different interstellar regions.[3,41,42]

High-resolution infrared spectroscopy has provided information on the excited vibrational states of HOC$^+$.[41] The infrared absorption of the ν_1 band was detected by Nakanaga and Amano in a hollow-cathode discharge in a mixture of CO and H$_2$.[43] Amano[44] suggested that the ν_2 frequency of HOC$^+$ is likely lower than 300 cm^{-1} from the observation of the $\nu_1 + \nu_2 - \nu_2$ combination band, suggesting that ν_2 is a large-amplitude motion. The pure rotational transitions in the ν_2 excited state of HOC$^+$ were investigated a few years later by Amano and Maeda.[45] No experimental information is available for the stretching ν_3 mode.

Several isotopologues of HCO$^+$ and HOC$^+$ were observed in the laboratory and in outer space,[1,9,33,46–50]

but not all of them. The situation with the rare isotopes is expected to change with the increasing sensitivity of receivers and large collecting areas. The Northern Extended Millimeter Array (NOEMA) radiotelescope will double the number of antennas (to twelve) by 2019, which will improve its spatial resolution and sensitivity, such that NOEMA will soon become the most advanced facility for millimeter radio astronomy in the Northern Hemisphere.[51] To fully exploit advanced facilities (such as Herschel, ALMA, SOFIA), spectroscopic studies over larger energy ranges are needed already now, in particular for molecular systems of astrophysical/astrochemical relevance, such as HCO^+.

In astrochemical models, isotope fractionation reactions were introduced to describe the enrichment of heavy isotopes in dark interstellar clouds.[52,53] These enrichment processes are also important in geochemistry.[54] The isotope fractionation reaction of HCO^+/HOC^+ with CO was a subject of our recent studies,[55,56] which provide new exothermicities and rate coefficients relevant for temperatures of dark interstellar cloud environments for all the isotopologues involving ^{12}C, ^{13}C, ^{16}O, ^{17}O, ^{18}O, H, and D. These results were obtained with the help of the global three-dimensional potential energy surface (PES) previously developed for the isomerizing system HCO^+/HOC^+ at the CCSD(T)/cc-pVQZ level of theory.[57] The localized HCO^+ and HOC^+ energy levels below the ground-state adiabatic isomerization barrier for $J = 0 - 2$ and all bound vibrational levels for $J = 0$ (in total 6042 bound states up to the first classical dissociation limit $H^+ + CO$ at 51 621 cm^{-1}) were studied for the CCSD(T)/cc-pVQZ PES in our original work.[57] A simple empirical model, developed there to simulate energy level pattern of isomerizing linear triatomic molecules, is useful for chemical models at high temperatures. To our knowledge, the CCSD(T)/cc-pVQZ potential energy surface remains the only available functional representation designed for both HCO^+ and HOC^+, based on higher-energy *ab initio* points, too. Its accuracy was documented previously.[57]

In the present work, we revisit the CCSD(T)/cc-pVQZ PES with the purpose of providing a spectroscopic characterization of the isotopologues of HCO^+ and HOC^+ by theoretical means. Quantum mechanical calculations of the rovibrational energies are performed by means of the DVR+DGB method (Section II). The computed energies are used to derive the parameters of the effective spectroscopic Hamiltonian (Section III A). Using the experimental ground-state rotational constants B_0 in combination with our theoretical rotation-vibration corrections (obtained beyond a perturbational approach), we additionally determine a new estimate for the equilibrium structure of both HCO^+ and HOC^+ (Section III B). Least-squares procedures for the linear and nonlinear fitting are used.[58]

Nominal abundances of carbon isotopes ^{12}C and ^{13}C are 98.90(3) and 1.10(3)%, nominal abundances of oxygen isotopes ^{16}O, ^{17}O, and ^{18}O are 99.762(15), 0.038(3),

and 0.200(12)%; and, finally, nominal abundances of H and D are 99.985(1) and 0.015(1)%, as given by Mills and coworkers.[59] In the present work, the mass numbers are stated for each of the elements in the chemical formulas only in Tables I-IV. In the rest of the text, we provide the isotope information in chemical formulas only if the isotope is not the most abundant.

II. THEORETICAL ASPECTS

In the calculations of the rovibrational energies of HCO^+/HOC^+, we have employed orthogonal (Jacobi) internal coordinates (r, R, θ) in the body-fixed formulation, where r is the CO bond length, R the distance from the proton to the center of mass of the C-O subunit, and θ the angle between the Jacobi vectors $\mathbf{r}$ and $\mathbf{R}$. The two-vector embedded body-fixed reference frame is chosen such that the body-fixed z-axis is aligned with the bond-distance vector $\mathbf{r}$.[60] The nuclear dynamics calculations were carried out by means of the discrete variable representation (DVR) for the angular coordinate in conjunction with real two-dimensional distributed Gaussian basis (DGB) functions for the radial degrees of freedom. Using a sequential diagonalization and basis-set truncation, the computational strategy leads to a very compact final rovibrational basis of relatively modest size. This approach is termed DVR+DGB and involves no dynamical approximation.[57,61]

We use the global three-dimensional potential energy surface developed for HCO^+/HOC^+ in its electronic ground state $(^1\Sigma^+)$ at the CCSD(T)/cc-pVQZ level of theory by Mladenović and Schmatz.[57] This is an isomerizing system with a bare barrier to isomerization at 26838 cm^{-1} (3.33 eV) relative to the global HCO^+ minimum. The isoformyl molecular ion, HOC^+, is 13876 cm^{-1} (1.72 eV) higher in energy than HCO^+. On this PES, the equilibrium distances of HCO^+ are $r_e(CH)$=1.0935 Å and $r_e(CO)$=1.1086 Å. For HOC^+, we have $r_e(HO)$=0.9904 Å and $r_e(CO)$=1.1579 Å.

For HCO^+/HOC^+ and DCO^+/DOC^+, we consider all the isotopic variants of ^{12}C, ^{13}C, ^{16}O, ^{17}O, and ^{18}O. The rovibrational calculations were carried out for the total rotational angular momentum J as high as $J = 15$ in both parities for each of the species (in total 24 species). Additional calculations were performed also for $J = 30$ for the purpose of verifying the derived spectroscopic constants.

III. RESULTS

The vibrational states of HCO^+ and HOC^+ are labelled by (v_1, v_2^ℓ, v_3), where v_1, v_3 are quantum numbers for the stretching ν_1, ν_3 vibrations and v_2 for the doubly degenerate bending ν_2 vibration. The vibrational angular momentum quantum number is ℓ. The total rotational quantum number J and parity p are strictly con-

served. The energy of the state $(\nu_1, \nu_2^\ell, \nu_3)$ is denoted by E_{v_1, v_2^ℓ, v_3} or E_{v_1, v_2, v_3}.

A. Spectroscopic parameters

We follow common practice of experiment. The rovibrational energies computed for a vibrational Σ state v are fitted to the standard polynomial expansion in $J(J+1)$,

$$
\begin{aligned}
E_v(J) =& T_v + B_v \, J(J+1) - D_v \, J^2(J+1)^2 \\
& + H_v \, J^3(J+1)^3 + \cdots .
\end{aligned}
\tag{1}
$$

For a Π state, we use the expansion

$$
\begin{aligned}
E_v(J) =& T_v + B_v \, \big[J(J+1) - \ell^2 \big] \\
& - D_v \, \big[J(J+1) - \ell^2 \big]^2 \\
& + H_v \, \big[J(J+1) - \ell^2 \big]^3 + \cdots \\
& \pm \tfrac{1}{2} \big[q_v \, J(J+1) + q_v^J \, J^2(J+1)^2 \\
& \qquad + q_v^{JJ} \, J^3(J+1)^3 + \cdots \big] .
\end{aligned}
\tag{2}
$$

In Eqs. (1) and (2), T_v is the term energy and B_v the effective rotational constant. The centrifugal distortion contribution is expressed in terms of the quartic centrifugal distortion constant D_v and the higher order constants, such as H_v (sextic), L_v (octic), and so on. The rotational dependence of the ℓ-type doubling contribution is described by a polynomial in $J(J+1)$, with q_v being the ℓ-type doubling constant. The parameters q_v^J, q_v^{JJ}, and so on are the centrifugal distortion corrections. Lattanzi et al.[1] also used the expansions of Eqs. (1) and (2) in their analysis of laboratory data on HCO^+, DCO^+, $H^{13}CO^+$, and $D^{13}CO^+$.

The spectroscopic parameters obtained in the fit for the vibrational ground state and the excited ν_1, ν_2 and ν_3 states are summarized in Tables I and II for the isotopic variants of HCO^+ and in Tables III and IV for the isotopic variants of HOC^+. Available experimental data are also given there. We use X_0, X_1, X_2, X_3 to denote the value of the parameter X in the vibrational states $(0,0^0,0)$, $(1,0^0,0)$, $(0,1^1,0)$, and $(0,0^0,1)$, respectively. The Π state $(0,1^1,0)$ is accessible for $J \geq 1$ only. It has two components of different parities, denoted by $(0,1^{1e},0)$ and $(0,1^{1f},0)$ in the convention of Brown et al.[66] for the labeling of parity doublet levels in linear molecules. In Eq. (2), the plus sign is used for the level $(0,1^{1f},0)$. The effective spectroscopic parameters of Eq. (2) reported for $(0,1^1,0)$ in Tables I-IV are computed by means of the two-step procedure employing

$$
\begin{aligned}
\frac{E_2^f(J) + E_2^e(J)}{2} =& T_2 + B_2 \, \big[J(J+1) - \ell^2 \big] \\
& - D_2 \, \big[J(J+1) - \ell^2 \big]^2 + \cdots
\end{aligned}
\tag{3}
$$

and

$$
\begin{aligned}
E_2^f(J) - E_2^e(J) =& q_2 \, J(J+1) + q_2^J \, J^2(J+1)^2 \\
& + q_2^{JJ} \, J^3(J+1)^3 + \cdots ,
\end{aligned}
\tag{4}
$$

where $E_2^f(J)$ and $E_2^e(J)$ are the energies of $(0,1^{1f},0)$ and $(0,1^{1e},0)$, respectively. In regular spectroscopic situations, $E_2^f(J) > E_2^e(J)$ holds.

In the fitting procedure, higher-order rotational Hamiltonians were also considered since we use high J values. The sixth-order spectroscopic Hamiltonian was found satisfactory to describe the rotational excitation in the vibrational states of HCO^+ in Table I and DCO^+ in Table II, except for the ν_1 state of DCO^+. To fit centrifugal distortion effects in ν_1 of DCO^+, terms higher than L_1 were necessary. In the case of HOC^+, terms up to L_v are used for the ground vibrational state, ν_1, and ν_2 and up to K_v for ν_3 in Table III. The terms up to K_v are used for all four states of DOC^+ in Table IV. The fit standard deviations σ in Tables I-IV are approximately 10 Hz. The maximum deviation is 22 Hz in Table I, 40 Hz in Table II, 37 Hz in Table III, and 13 Hz in Table IV. The fitted rotational energies are up to approximately 350 cm^{-1} (about 10 THz) for $J = 15$.

Combining microwave data coming from different experimental groups, Lattanzi et al.[1] derived the spectroscopic parameters for the ground vibrational state of HCO^+, which include a large, negative sextic centrifugal distortion constant, $H_0 = -0.341(156)$ Hz. This finding for H_0 led Tinti et al.[12] to reinvestigate the rotational transitions of HCO^+, reporting $H_0 = 0.083(36)$ Hz with an uncertainty of 43%. Cazzoli et al.[13] recorded the rotational transitions in the frequency range 1-1.6 THz and derived $H_0 = 0.0774(58)$ Hz with an uncertainty of 7.5% in their Fit 2. Including the octic centrifugal distortion constant (Fit 1), they found $H_0 = 0.137(46)$ Hz and $L_0 = -0.118(91)$ mHz, so that H_0 with an uncertainty of 34% became less accurate. Since Cazzoli et al.[13] suggested that Fit 2 is more reliable than Fit 1, we quote their values from Fit 2 in Table I. These authors also reported the equilibrium sextic centrifugal distortion constant $H_e = 0.060$ Hz, obtained by the vibrational second-order perturbational approach at the CCSD(T)/aug-cc-pCV5Z level of theory.

The sextic centrifugal distortion constant H_0 for the ground vibrational state of HCO^+ in Table I is explicitly $H_0 = 0.0711171(59)$ Hz, where the uncertainty in the last digits quoted in parentheses is one standard deviation. To test the quality of our H_0, we included $J = 20$ and $J = 30$ transitions in the fitting procedure, yielding $H_0 = 0.07071(1)$ Hz with $\sigma_0 = 506$ Hz for the sixth-order rotational representation and $H_0 = 0.0712989(4)$ Hz, $L_0 = -0.0004022(3)$ mHz, and $\sigma_0 = 1.41$ Hz for the eighth-order rotational representation. The latter H_0 value and H_0 from Table I differ by 0.00018 Hz (0.25%). The difference between our H_0 and the result of Cazzoli et al.[13] is 0.006 Hz (less than 10%).

Individual standard deviations of the fitting param-

TABLE I: Spectroscopic parameters for the isotopic variants of HCO^+. Experimental values are given in brackets.

Parameter	$H^{12}C^{16}O^+$	$H^{12}C^{17}O^+$	$H^{12}C^{18}O^+$	$H^{13}C^{16}O^+$	$H^{13}C^{17}O^+$	$H^{13}C^{18}O^+$
B_0 / MHz	44376.28	43315.62	42372.29	43164.34	42087.62	41129.91
D_0 / kHz	81.95	78.10	74.76	77.59	73.80	70.51
	$[82.83]^a$	$[79.08]^b$		$[78.41]^c$		
H_0 / Hz	0.071	0.065	0.061	0.063	0.058	0.053
	$[0.077]^a$					
σ_0 / Hz	8.45	9.03	7.64	8.52	7.63	6.67
ΔB_0 / MHz	243.73	235.44	228.15	234.10	225.80	218.50
B_0^{est} / MHz	44594.42	43528.77	42580.99	43377.18	42295.37	41333.14
	$[44594.43]^a$	$[43528.93]^b$	$[42581.21]^d$	$[43377.30]^c$		$[41333.59]^e$
T_2 /cm^{-1}	829.25	828.21	827.29	821.80	820.75	819.82
	$[828.23]^c$					
B_2 / MHz	44456.45	43393.39	42447.94	43235.29	42156.31	41196.62
D_2 / kHz	83.57	79.62	76.19	79.01	75.13	71.76
	$[84.49^c,84.44^g]$					
H_2 / Hz	0.084	0.077	0.071	0.074	0.067	0.062
σ_2 / Hz	11.45	10.43	8.69	9.37	8.69	7.58
q_2 / MHz	209.85	200.21	191.82	200.36	190.75	182.40
	$[211.76^f,211.78^g]$					
q_2^J / kHz	-1.79	-1.67	-1.56	-1.65	-1.53	-1.42
	$[-1.73^f,-1.83^g]$					
q_2^{JJ} / Hz	0.024	0.021	0.019	0.020	0.018	0.016
σ_q / Hz	9.14	7.36	6.62	11.55	7.07	8.66
α_2 / MHz	-80.17	-77.77	-75.66	-70.95	-68.69	-66.70
B_2^{est} / MHz	44674.59	43606.54	42656.65	43448.13	42364.07	41399.84
	$[44677.15^{c,f},44676.97^g]$		$[42659.16]^e$	$[43450.52]^e$		$[41402.39]^e$
T_3 /cm^{-1}	2179.09	2152.31	2128.19	2145.35	2117.55	2092.51
	$[2183.95]^c$					
B_3 / MHz	44083.69	43032.70	42097.95	42880.92	41814.02	40865.01
D_3 / kHz	82.04	78.18	74.83	77.69	73.89	70.59
	$[82.90]^g$					
H_3 / Hz	0.070	0.065	0.060	0.062	0.057	0.053
σ_3 / Hz	7.51	7.09	6.05	7.07	6.23	5.65
α_3 / MHz	292.59	282.91	274.34	283.42	273.60	264.90
B_3^{est} / MHz	44301.83	43245.85	42306.65	43093.76	42021.77	41068.24
	$[44299.87]^{c,g}$		$[42305.02]^e$	$[43091.85]^e$		
T_1 /cm^{-1}	3085.58	3083.08	3080.96	3062.99	3060.86	3059.05
	$[3088.74]^c$					
B_1 / MHz	44023.87	42972.11	42037.62	42836.68	41769.75	40821.17
D_1 / kHz	81.22	77.42	74.11	76.98	73.20	69.93
	$[82.09^f,82.06^g]$					
H_1 / Hz	0.068	0.065	0.061	0.062	0.058	0.054
σ_1 / Hz	14.70	13.02	10.42	9.29	9.19	9.37
α_1 / MHz	352.41	343.51	334.67	327.66	317.87	308.74
B_1^{est} / MHz	44242.01	43185.26	42246.32	43049.52	41977.50	41024.39
	$[44240.53]^{f,g}$		$[42244.86]^e$	$[43048.16]^e$		

^{a} Fit 2 of Cazzoli et al.[13]
^{b} Dore et al.[49]
^{c} Lattanzi et al.[1]
^{d} Bogey et al.[9]
^{e} taken from Puzzarini et al.[62]
^{f} Neese et al.[21]
^{g} Hirao et al.[63]

TABLE II: Spectroscopic parameters for the isotopic variants of DCO$^+$. Experimental values are given in brackets.

Parameter	D^{12}C^{16}O$^+$	D^{12}C^{17}O$^+$	D^{12}C^{18}O$^+$	D^{13}C^{16}O$^+$	D^{13}C^{17}O$^+$	D^{13}C^{18}O$^+$
B_0 / MHz	35851.81	35006.52	34252.67	35201.11	34339.34	33570.60
D_0 / kHz	55.21	52.49	50.13	52.85	50.16	47.83
	[55.80]^{a,b}		[50.67]^b	[53.41]^{a,b}		
H_0 / Hz	0.050	0.046	0.043	0.046	0.043	0.040
	[0.052^a,0.054^b]		[0.11]^b	[0.042^a,0.048^b]		
σ_0 / Hz	6.56	6.16	5.62	5.74	5.05	3.81
ΔB_0 / MHz	173.53	167.61	162.40	168.75	162.78	157.52
B_0^{est} / MHz	36019.81	35170.82	34413.66	35366.70	34501.13	33729.00
	[36019.77]^{a,b}		[34413.79]^b	[35366.71]^{a,b}		
T_2 /cm^{-1}	666.30	664.98	663.81	656.85	655.51	654.33
	[666±3]^c					
B_2 / MHz	35946.99	35099.19	34343.11	35288.40	34424.21	33653.32
D_2 / kHz	56.82	54.00	51.56	54.30	51.52	49.11
	[57.52^a,57.41^d]					
H_2 / Hz	0.063	0.058	0.054	0.058	0.053	0.049
σ_2 / Hz	12.29	9.29	9.25	8.60	8.83	10.38
q_2 / MHz	169.56	161.98	155.36	165.76	158.07	151.35
	[171.02^a,170.99^d]					
q_2^J / kHz	-1.32	-1.23	-1.15	-1.25	-1.16	-1.08
	[-1.84^a,-1.29^d]					
q_2^{JJ} / Hz	0.023	0.021	0.019	0.020	0.018	0.016
σ_q / Hz	5.05	7.90	4.07	6.73	5.28	11.54
α_2 / MHz	-95.18	-92.68	-90.45	-87.29	-84.87	-82.72
B_2^{est} / MHz	36115.00	35263.50	34504.10	35453.99	34586.00	33811.72
	[36116.79^a,36116.67^d]					
T_3 /cm^{-1}	1900.81	1885.26	1870.75	1893.85	1877.24	1861.73
	[1904.06]^a					
B_3 / MHz	35646.33	34809.36	34062.72	35003.43	34149.75	33388.01
D_3 / kHz	55.18	52.45	50.09	52.81	50.12	47.78
	[55.58]^a					
H_3 / Hz	0.049	0.045	0.043	0.044	0.042	0.039
σ_3 / Hz	2.44	3.07	3.23	3.29	1.42	3.84
α_3 / MHz	205.48	197.16	189.94	197.69	189.59	182.59
B_3^{est} / MHz	35814.34	34973.67	34223.71	35169.01	34311.54	33546.41
	[35813.35]^{a,d}					
T_1 /cm^{-1}	2580.46	2566.34	2554.23	2529.47	2515.77	2504.09
	[2584.56]^a					
B_1 / MHz	35626.92	34766.94	34001.31	34835.62	33975.49	33199.35
D_1 / kHz	46.05	41.38	40.52	40.28	32.04	14.39
	[46.36]^a					
H_1 / Hz	-2.441	-1.051	0.040	-4.010	-7.542	-21.207
L_1 / mHz	0.326	-0.234	-0.199	1.566	3.765	15.944
K_1 /μHz	0.037	0.081	0.004	-0.697	-1.974	-11.878
M_1 / nHz				0.300	0.797	5.932
σ_1 / Hz	3.92	6.83	3.17	9.76	16.40	30.07
α_1 / MHz	224.89	239.58	251.36	365.50	363.85	371.25
B_1^{est} / MHz	35794.93	34931.25	34162.30	35001.20	34137.28	33357.74
	[35792.33]^{a,d}					

^{a} Lattanzi et al.[1]
^{b} Caselli and Dore.[50]
^{c} Foltynowicz et al.[64]
^{d} Hirao et al.[65]

eters in Tables I-IV are not listed for brevity. For a given model, the vast majority of the parameters are found to be statistically well-defined, with an uncertainty of less than 1%. All the parameters for the isotopic variants of HCO$^+$ in Table I have an uncertainty of less than 0.1%. Uncertainties of three parameters in Table II, five in Table III, and three in Table IV are larger than 5%. In Table II, for instance, these are K_1(DC^{18}O$^+$)=0.0041(7) μHz, M_1(D^{13}CO$^+$)=0.300(40) nHz, and M_1(D^{13}C^{17}O$^+$)=0.797(67) nHz.

For all the systems in Tables I-IV, we additionally calculated the rovibrational energies for $J = 30$ in both parities and compared them with the predictions from the term formulas. We found an agreement better than 1 MHz for all 24 systems in the vibrational ground state, as well as for HCO$^+$ and DCO$^+$ in the excited ν_2 and ν_3 states. For the HOC$^+$ and DOC$^+$ forms in the excited ν_1, ν_2, and ν_3 states, the agreement is within 17 and 7 MHz, respectively. The rotational excitation in the ν_1 state of the D^{12}CO$^+$ forms is predicted better than 10 MHz. For D^{13}C^{16}O$^+$, D^{13}C^{17}O$^+$, and D^{13}C^{18}O$^+$ in the excited ν_1 state, the agreement is within 40, 75, and 625 MHz. The less satisfactory performance in the latter three cases is an indication of more complex internal dynamics. The $J = 30$ rotational energies correspond to approximately 1400 cm^{-1} (about 40 THz).

B. Equilibrium structure

The rotational constants B_0, B_1, B_2, B_3 in Tables I-IV are approximately 200 MHz smaller than the experimental values. These discrepancies arise primarily from the equilibrium distances, found to be slightly too long (approximately 0.2-0.3 %) for the CCSD(T)/cc-pVQZ potential energy surface.[57]

In the traditional spectroscopic approach,[67] the rovibrational correction S_{v_1,v_2,v_3} to the equilibrium rotational constant B_e is given by

$$S_{v_1,v_2,v_3} = B_e - B_{v_1,v_2,v_3} = \sum_{i=1}^{3} \alpha_i \left(v_i + \frac{d_i}{2} \right), \quad (5)$$

where α_i is a vibration-rotation interaction constant for the ith vibrational mode with the degree of degeneracy d_i, in fact

$$\alpha_1 = B_{0,0,0} - B_{1,0,0}, \quad \alpha_2 = B_{0,0,0} - B_{0,1,0}, \quad \text{and} \quad \alpha_3 = B_{0,0,0} - B_{0,0,1}. \quad (6)$$

For the ground vibrational state, this gives

$$S_0 = \tfrac{1}{2} \left(\alpha_1 + 2\alpha_2 + \alpha_3 \right), \quad (7)$$

so that

$$B_i = B_e - S_0 - \alpha_i \quad \text{for} \quad i = 1, 2, 3. \quad (8)$$

From our calculations, on the other hand, we have

$$\Delta B_0 = B_e^{th} - B_0^{th}, \quad (9)$$

where B_e^{th} and B_0^{th} are theoretical values of the rotational constant at equilibrium and in the ground vibrational state, respectively. Thus

$$B_i^{th} = B_e^{th} - \Delta B_0 - \alpha_i^{th} \quad \text{for} \quad i = 1, 2, 3, \quad (10)$$

where $\alpha_i^{th} = B_0^{th} - B_i^{th}$. The equilibrium rotational constant B_e^{th} provides the major contribution to B_i^{th} in Eq. (10). Replacing B_e^{th} with another value B_e^{est}, we obtain new estimates for the ground state rotational constant, B_0^{est}, and for the rotational constant in the excited ith vibrational mode, B_i^{est}, as follows

$$B_0^{est} = B_e^{est} - \Delta B_0 \quad \text{and} \quad B_i^{est} = B_e^{est} - \Delta B_0 - \alpha_i^{th}, \quad (11)$$

respectively. Hereby we assume that ΔB_0 and α_i^{th} are unchanged with respect to Eqs. (9) and (10), in fact that the coupling between the overall rotation and vibrations is well described by the computational approach employed. To obtain good estimates B_i^{est} in Eq. (11), we need a best possible estimate B_e^{est}. In Tables I-IV, the theoretical values B_i^{th} and α_i^{th} are shown without the superscript.

The experimental ground state rotational constants B_0^{exp} are available for HCO$^+$, HC^{17}O$^+$, HC^{18}O$^+$, H^{13}CO$^+$, and H^{13}C^{18}O$^+$ (Table I), as well as for DCO$^+$, DC^{18}O$^+$, and D^{13}CO$^+$ (Table II). Combining the experimental B_0^{exp} values with our vibration-rotation corrections ΔB_0, so that

$$B_e^{est} = B_0^{exp} + \Delta B_0, \quad (12)$$

we determined from eight B_e^{est} values the equilibrium distances r_e(CH) and r_e(CO) of HCO$^+$ by means of a nonlinear least-squares technique (the Levenberg-Marquardt algorithm). The calculated distances r_e(CH) and r_e(CO) are listed in Table V, along with the values recommended by Botschwina et al.,[68] Puzzarini et al.,[62] and Dore et al.[69] The equilibrium distances due to Puzzarini et al.[62] are quoted there with the uncertainty of one standard deviation, as given also in Ref. 69. Dore et al.[69] derived the equilibrium structure of HCO$^+$ from the millimeter wave spectroscopy data for the four species HCO$^+$, DCO$^+$, H^{13}CO$^+$, and HC^{18}O$^+$. In our Fit 4, we employ the data from Tables I and II only for these four systems. Our results in Table V agree nicely with the experimental values of Dore and coworkers,[69] with our r_e(CH) distance being shorter by 6×10^{-5} Å and r_e(CO) longer by 3.5×10^{-5} Å. The agreement of the corresponding B_e constants is within 1.6 MHz. Table V provides also the equilibrium structure computed by Czakó et al.[70] at the all electron CCSD(T)/aug-cc-pCVQZ level of theory. Compared to the results of Dore et al.[69] and found here, the theoretical r_e(CH) and r_e(CO) values of Czakó et al.[70] are both longer, r_e(CH) by 5×10^{-4} Å and r_e(CO) by 1×10^{-3} Å, whereas B_e is smaller by 74 MHz.

The equilibrium structure of HOC$^+$ was a subject of controversy. From the observation of the isotopic variants H^{18}OC$^+$ and HO^{13}C$^+$, Gudeman and Woods[33] derived a

TABLE III: Spectroscopic parameters for the isotopic variants of HOC$^+$. Experimental values are given in brackets.

Parameter	H^{16}O^{12}C$^+$	H^{17}O^{12}C$^+$	H^{18}O^{12}C$^+$	H^{16}O^{13}C$^+$	H^{17}O^{13}C$^+$	H^{18}O^{13}C$^+$
B_0 / MHz	44510.75	43757.35	43078.22	42652.08	41884.71	41192.97
D_0 / kHz	113.76 [114.57]^a	109.59	105.96	104.17	100.14	96.64
H_0 / Hz	0.760 [2.12]^a	0.658	0.579	0.620	0.526	0.458
L_0 / mHz	-0.046	-0.038	-0.032	-0.035	-0.028	-0.023
σ_0 / Hz	4.30	3.66	2.99	2.76	3.18	2.36
ΔB_0 / MHz	42.57	54.65	65.13	44.20	55.75	65.71
B_0^{est} / MHz	44743.93 [44743.91]^a	43987.56	43305.74 [43305.99]^b	42876.39 [42876.56]^b	42105.94	41411.39
T_2 /cm^{-1}	243.60	242.26	241.08	243.22	241.89	240.71
B_2 / MHz	44705.05	43933.78	43239.03	42831.80	42047.22	41340.39
D_2 / kHz	116.15 [117.23]^a	111.68	107.78	106.30	102.04	98.31
H_2 / Hz	0.284	0.226	0.177	0.229	0.186	0.147
L_2 / mHz	0.028	0.027	0.026	0.018	0.019	0.018
σ_2 / Hz	8.38	7.84	6.77	3.57	4.61	6.12
q_2 / MHz	517.07 [518.77]^a	502.44	489.34	475.81	461.30	448.38
q_2^J / kHz	-20.66 [-20.48]^a	-19.07	-17.72	-17.84	-16.35	-15.12
q_2^{JJ} / Hz	1.484	1.326	1.204	1.196	1.054	0.949
q_2^{JJJ} / mHz	-0.150	-0.132	-0.118	-0.105	-0.095	-0.087
q_2^{JJJJ} / μHz	0.016	0.015	0.012	0.008	0.008	0.012
σ_q / Hz	2.40	1.17	1.60	1.92	1.62	3.57
α_2 / MHz	-194.30	-176.43	-160.80	-179.72	-162.51	-147.42
B_2^{est} / MHz	44938.23 [44939.79]^a	44163.99	43466.54	43056.12	42268.46	41558.81
T_3 /cm^{-1}	1901.32	1880.68	1862.01	1858.64	1837.41	1818.20
B_3 / MHz	44152.59	43406.90	42734.72	42314.73	41555.11	40870.41
D_3 / kHz	115.39	111.06	107.30	105.45	101.30	97.72
H_3 / Hz	1.066	0.859	0.725	0.715	0.612	0.528
L_3 / mHz	-0.251	-0.142	-0.091	-0.057	-0.047	-0.037
K_3 /μHz	0.119	0.054	0.026	0.007	0.005	0.005
σ_3 / Hz	8.36	4.19	3.43	7.06	5.64	3.01
α_3 / MHz	358.16	350.45	343.50	337.35	329.60	322.56
B_3^{est} / MHz	44385.77	43637.11	42962.23	42539.05	41776.34	41088.83
T_1 /cm^{-1}	3276.54 [3268.03]^c	3269.21	3262.83	3276.14	3268.78	3262.43
B_1 / MHz	44226.48	43487.88	42821.85	42385.97	41632.26	40953.21
D_1 / kHz	115.01 [116.4]^c	110.57	106.81	105.58	100.93	97.28
H_1 / Hz	1.045	0.893	0.820	0.863	0.713	0.628
L_1 / mHz	-0.067	-0.055	-0.058	-0.013	-0.040	-0.035
σ_1 / Hz	14.12	5.05	12.65	23.52	10.85	3.64
α_1 / MHz	284.27	269.47	256.37	266.11	252.45	239.76
B_1^{est} / MHz	44459.65 [44457.10]^c	43718.10	43049.36	42610.28	41853.49	41171.63

^{a} Amano and Maeda.[45]
^{b} calculated from the transition $J = 0 \to 1$ observed by Gudeman and Woods.[33,34]
^{c} Nakanaga and Amano.[43]

preliminary substituted r_s structure of HOC$^+$, with the substitution bond lengths equal to $r_s(\text{CO}) = 1.1595$ Å and $r_s(\text{OH}) = 0.9342$ Å. Compared to available theoretical values,[72] $r_e(\text{CO}) = 1.1536$ Å and $r_e(\text{OH}) = 0.9892$ Å,

the result for $r_s(\text{OH})$ appeared to be too short. This discrepancy has been ascribed to a very low-frequency bending mode. Gudeman and Woods[33] also suspected that the bending potential of HOC$^+$ may possibly be

TABLE IV: Spectroscopic parameters for the isotopic variants of DOC$^+$. Experimental values are given in brackets.

Parameter	D^{16}O^{12}C$^+$	D^{17}O^{12}C$^+$	D^{18}O^{12}C$^+$	D^{16}O^{13}C$^+$	D^{17}O^{13}C$^+$	D^{18}O^{13}C$^+$
B_0 / MHz	38013.93	37570.59	37166.05	36472.02	36012.45	35593.01
D_0 / kHz	93.59	90.40	87.60	85.27	82.21	79.52
	[93.86]^a					
H_0 / Hz	2.305	2.100	1.925	1.896	1.716	1.564
	[2.15]^a					
L_0 / mHz	-0.245	-0.217	-0.193	-0.188	-0.165	-0.147
K_0 /μHz	0.026	0.022	0.018	0.018	0.016	0.014
σ_0 / Hz	0.88	0.90	1.13	1.08	1.35	1.00
ΔB_0 / MHz	-146.99	-132.31	-119.25	-137.33	-123.03	-110.33
B_0^{est} / MHz	38193.18	37748.78	37343.26	36645.09	36184.37	35763.86
	[38193.20]^a					
T_2 /cm^{-1}	176.57	174.88	173.37	176.06	174.36	172.86
B_2 / MHz	38338.54	37877.02	37456.30	36777.25	36299.86	35864.58
D_2 / kHz	100.63	96.79	93.44	91.51	87.85	84.65
H_2 / Hz	1.734	1.543	1.382	1.429	1.261	1.119
L_2 / mHz	-0.049	-0.036	-0.027	-0.039	-0.029	-0.017
K_2 /μHz	-0.012	-0.011	-0.010	-0.007	-0.006	-0.009
σ_2 / Hz	1.02	1.22	0.70	0.99	1.40	0.53
q_2 / MHz	512.16	505.01	498.38	473.08	465.62	458.72
q_2^J / kHz	-31.90	-30.35	-28.95	-27.86	-26.40	-25.09
q_2^{JJ} / Hz	3.024	2.813	2.631	2.481	2.297	2.140
q_2^{JJJ} / mHz	-0.378	-0.346	-0.318	-0.288	-0.263	-0.246
q_2^{JJJJ} / μHz	0.056	0.048	0.043	0.039	0.034	0.034
σ_q / Hz	1.74	1.42	1.61	1.72	1.84	1.48
α_2 / MHz	-324.61	-306.43	-290.25	-305.23	-287.42	-271.57
B_2^{est} / MHz	38517.78	38055.22	37633.51	36950.33	36471.78	36035.43
T_3 /cm^{-1}	1839.77	1826.19	1813.48	1800.12	1785.61	1772.06
B_3 / MHz	37753.34	37314.77	36914.28	36225.78	35770.95	35355.57
D_3 / kHz	94.01	91.10	88.50	85.72	82.88	80.36
H_3 / Hz	2.352	2.180	2.029	1.941	1.787	1.652
L_3 / mHz	-0.250	-0.228	-0.207	-0.189	-0.173	-0.156
K_3 /μHz	0.023	0.024	0.020	0.011	0.015	0.013
σ_3 / Hz	5.76	3.21	1.64	8.91	2.72	3.74
α_3 / MHz	260.59	255.83	251.77	246.23	241.50	237.45
B_3^{est} / MHz	37932.58	37492.96	37091.50	36398.86	35942.87	35526.41
T_1 /cm^{-1}	2482.93	2467.11	2453.43	2478.97	2463.55	2450.23
B_1 / MHz	37718.13	37285.03	36890.03	36191.94	35742.86	35333.10
D_1 / kHz	99.88	95.84	92.34	90.66	86.84	83.54
H_1 / Hz	3.434	3.061	2.758	2.801	2.486	2.229
L_1 / mHz	-0.425	-0.367	-0.316	-0.327	-0.280	-0.244
K_1 /μHz	0.058	0.046	0.036	0.037	0.032	0.027
σ_1 / Hz	3.84	4.73	4.28	7.21	5.20	3.41
α_1 / MHz	295.80	285.56	276.02	280.08	269.59	259.92
B_1^{est} / MHz	37897.37	37463.23	37067.24	36365.02	35914.78	35503.94

^{a} Amano and Maeda.[45]

quasilinear. The calculations of Kraemer and Bunker[73] showed that HOC$^+$ is not quasilinear, but linear with a very shallow bending potential.

To derive the equilibrium structure of HOC$^+$, we employ the ground-state rotational constants for HOC$^+$ and DOC$^+$ due to Amano and Maeda.[45] From the $J = 0 \rightarrow 1$ transition, observed for HO^{13}C$^+$ and H^{18}OC$^+$ by Gudeman and Woods,[33,34] we derive the rotational constant B_0 from

$$\Delta E_0^1 = 2\,B_0 - 4\,D_0, \qquad (13)$$

where ΔE_0^1 stands for the lowest transition. For D_0, we employ our result from Table III. The values obtained with the help of Eq. (13) are listed in Table III as experimental B_0 results for HO^{13}C$^+$ and H^{18}OC$^+$. The computed equilibrium distances r_e(HO) and r_e(CO) are provided in Table V. In Fit 2, we use only the experimental B_0 values reported by Amano and Maeda.[45]

TABLE V: Equilibrium distances (in Å) and equilibrium rotational constants (in MHz) of HCO^+ and HOC^+.[a]

HCO^+	r_e(CH)	r_e(CO)	B_e(HCO^+)
This work	1.091 981(7)	1.105 615(2)	44 838.2
This work, Fit 4	1.091 989(1)	1.105 6137(3)	44 838.2
Dore et al.[69]	1.092 04	1.105 58	44 839.8
Puzzarini et al.[62]	1.091 9(3)	1.105 5(1)	44 847.1
Botschwina et al.[68]	1.091 9	1.105 8	44 826.7
Czakó et al.[70]	1.092 5	1.106 6	44 764.4
HOC^+	r_e(HO)	r_e(CO)	B_e(HOC^+)
This work	0.990 482(7)	1.154 468(2)	44 786.5
This work, Fit 2	0.990 478	1.154 469	44 786.5
Botschwina et al.[68]	0.988 5	1.154 6	44 800.3
Martin et al.[71]	0.988 17	1.154 71	44 796.6

[a] Values in parentheses show one standard error to the last significant digits of the distances.

The best estimate of Martin et al.[71] and the values recommended by Botschwina et al.[68] are also shown. Our finding agrees with the results from Refs. 68,71 within 0.002 Å and 0.0001-0.0002 Å for r_e(HO) and r_e(CO), respectively.

The equilibrium structures of Table V for HCO^+ and HOC^+ are used to compute the best estimates B_e^{est} of the equilibrum rotational constants. Having derived B_e^{est}, the best estimates B_i^{est} of the effective rotational constant for the ith fundamental vibration are calculated using Eq. (11). The values of B_i^{est} are given in Tables I-IV, where we also list the theoretical vibration-rotation constants $\alpha_1, \alpha_2, \alpha_3$. As seen, our B_2^{est} values are smaller and B_1^{est}, B_3^{est} larger by at most 3 MHz than the experimental results.

Additional note is needed regarding the procedure we use to derive the equilibrium structure of HCO^+ and HOC^+. We compute the equilibrium distances by nonlinear least-squares fittings of B_e^{est}, computed from the experimental B_0^{exp} and theoretical $\Delta B_0 = B_e^{th} - B_0^{th}$ values. Each of the input data was associated with a standard deviation σ_{esp}. Experimental standard deviations σ_e for B_0^{exp} are known from the literature,[1,9,13,33,34,45,49,50,62] varying from 0.00016 MHz to 0.060 MHz. For standard deviations σ_Δ of ΔB_0, we used standard deviations of our B_0 values, which are in order of 10^{-7} MHz and thus much smaller than σ_e. Herewith the description of our mathematical model is completed. The equilibrium distances shown in Table V should be viewed as the least-squares solutions to this well-postulated mathematical problem. The standard deviations in order of 10^{-6} Å in Table V are a mathematical (quantitative) measure of the accuracy of r_e with respect to the model used. The accuracy of our

model is defined by the accuracy of the experimental data coming from different sources and the accuracy of the CCSD(T)/cc-pVQZ potential energy surface. The PES does not include effects beyond the Born-Oppenheimer approximation or relativistic corrections. This deficiency, however, poses no major problem since we use the PES only to determine ΔB_0. We expect small change of excluded electronic-structure contributions over the coordinate range relevant in our calculations. Good agreement of our results with known experimental data in Tables I-III supports this statement. To exemplify the changes of the equilibrium rotational constant with the equilibrium distances reported so far, we provide also the corresponding B_e values in Table V.

IV. FINAL REMARKS

In the present work, we employed a pure ab initio potential energy surface in combination with the exact kinetic energy operator and an efficient numerical approach to calculate the rovibrational energies of HCO^+ and HOC^+ for $J = 0 - 15$. Fitting them to appropriate spectroscopic formulae, we derived the theoretical spectroscopic parameters, including higher-order centrifugal distortion constants. Since the fit standard deviations are approximately 10 Hz ($3 \cdot 10^{-10}$ cm^{-1}), the spectroscopic parameters provide a compact representation of the calculated rovibrational energies and allow for a quick comparison with experiment. This type of analysis was carried out for each of the isotopologues of HCO^+ and HOC^+ involving H, D, ^{16}O, ^{17}O, ^{18}O, ^{12}C, and ^{13}C. As such, these results form a consistent set of data. Combining the experimental B_0 rotational constants with our vibration-rotation corrections ΔB_0 for the ground vibrational state, we additionally derived the equilibrium structures of HCO^+ and HOC^+.

In experimental approaches, the vibration-rotation interaction constants $\alpha_1, \alpha_2, \alpha_3$ are used to determine the vibration-rotation correction S_0 of Eq. (7) in the ground vibrational state. For small-amplitude vibrations (rigid molecular systems), $S_0 \approx \Delta B_0$ holds. In other cases, the use of S_0 may lead to the equilibrium structure inconsistency problem. This was reported by Dore et al.[69,74] for the case of the formyl cation. These authors invoked the vibration-rotation Coriolis interaction to deperturb the state $(1, 0, 0)$ involved in their description in the Coriolis coupling with $(0, 1^1, 1)$, most strongly exhibited in DCO^+. Inclusion of additional terms into the effective spectroscopic Hamiltonian is a standard procedure for improving the spectroscopic model, effectively based on the harmonic-oscillator-rigid-rotor description as a zero-order picture. We only note that the Coriolis coupling term in our calculations plays an ordinary (usual) role in the overall internal dynamics of the formyl cation at lower energies.[57]

From the experimental B_i^{exp} values listed in Table II for DCO^+, one finds using the expression of Eq. (6)

that the experimental vibration-rotation interaction constants are $\alpha_1^{exp} = 227.44\,\text{MHz}$, $\alpha_2^{exp} = -96.9\,\text{MHz}$, and $\alpha_3^{exp} = 206.42\,\text{MHz}$. They agree with our α_i results within 2.6 MHz. From α_i^{exp} and α_i, we calculate $S_0^{exp} = 120.03\,\text{MHz}$ and $S_0 = 120.01\,\text{MHz}$ according to Eq. (7). These S_0 values are smaller by 53.5 MHz than $\Delta B_0(\text{DCO}^+)=173.53\,\text{MHz}$ in Table II. For the other species involved in our fitting procedure, the difference $\Delta B_0 - S_0$ amounts to 32.2 and -25.5 MHz for DC^{18}O^+ and D^{13}CO^+, respectively, whereas it varies from -1.6 to 1.5 MHz for the hydrogen-containing forms. This is clear evidence for somewhat different internal dynamics in the HCO^+ and DCO^+ isotopologues.

To extract information about the equilibrium structure from the experimental rotational B_0 constants, we actually need the quantity ΔB_0. This information as such is not accessible to experiment in an easy fashion. In perturbational approaches, B_0 is computed as the vibrationally averaged rotational constant by using some (rigid-rotor) formula for the rotational constant or as $B_e - S_0$. Due to this inherent problem, the perturbatively computed ΔB_0 values are at best of a semi-quantitative nature. We are thus left with the variational method as the only approach capable of providing well-founded ΔB_0 values that may assist experiment in the evaluation of the equilibrium structure. This is the line of reasoning followed in the present work. As we go further away from rigid molecular systems, this reasoning becomes even more important. In the case of larger systems, where the full-dimensional variational calculation is currently out of reach, we may use a reduced-dimensionality description of the internal motion to obtain variationally computed ΔB_0 values. In the reduced-dimensionality description, one combines as accurate as possible representations for those degrees of freedom dominating the internal dynamics with a simpler (even harmonic) picture for the other (kineticly inactive) modes. Descriptions of this type are successfully used for weakly bound complexes.

The rovibrational calculations presented in this work were carried out using the atomic masses (given by Mills et al.[59]). This is common practice in quantum mechanical considerations of the internal molecular motion. In the framework of the Born-Oppenheimer approximation, the nuclear motion should, strictly speaking, involve the nuclear masses. To investigate the influence of the atomic versus nuclear masses on the rovibrational states of $\text{HCO}^+/\text{HOC}^+$, we performed two test calculations. These results are summarized in Table VI. In Test 1 we replaced $m(H)$ with the proton mass and in Test 2 we used the nuclear masses of H, C, and O. The reference computation with the atomic masses is denoted as Test 0. The test calculations were carried out for $J = 0$ and $J = 1$ only. The properties, we compare in Table VI,

TABLE VI: Selected results for HCO^+ and HOC^+ from the rovibrational ($J = 0, 1$) DVR-DGB calculations employing the atomic masses (Test 0), the proton mass in combination with the atomic masses for carbon and oxygen (Test 1), and the nuclear masses (Test 2).

| | HCO^+ | | |
Property	Test 0	Test 1	Test 2
$\widetilde{\nu}_1$ / cm^{-1}	3085.58	3086.20	3086.29
$\widetilde{\nu}_2$ / cm^{-1}	830.72	830.88	830.91
$\widetilde{\nu}_3$ / cm^{-1}	2179.09	2179.20	2179.44
$\widetilde{q}_2$ / MHz	209.85	209.86	209.94
$\widetilde{B}_0$ / MHz	44376.11	44382.06	44391.21
$\widetilde{B}_1$ / MHz	44023.71	44029.62	44038.64
$\widetilde{B}_3$ / MHz	44083.53	44089.39	44098.46

| | HOC^+ | | |
Property	Test 0	Test 1	Test 2
$\widetilde{\nu}_1$ / cm^{-1}	3276.54	3277.30	3277.34
$\widetilde{\nu}_2$ / cm^{-1}	245.07	245.14	245.15
$\widetilde{\nu}_3$ / cm^{-1}	1901.32	1901.34	1901.59
$\widetilde{q}_2$ / MHz	517.00	516.96	517.18
$\widetilde{B}_0$ / MHz	44510.53	44514.78	44524.84
$\widetilde{B}_1$ / MHz	44226.43	44230.69	44240.61
$\widetilde{B}_3$ / MHz	44152.40	44156.58	44166.53

are

$$
\begin{aligned}
\widetilde{\nu}_i &= E_i(J = 0) - E_0(J = 0) \quad \text{for} \quad i = 1, 3, \\
\widetilde{\nu}_2 &= E_2^e(J = 1) - E_0(J = 0), \\
\widetilde{q}_2 &= \tfrac{1}{2}\left[E_2^f(J = 1) - E_2^e(J = 1) \right], \quad \text{and} \\
\widetilde{B}_i &= \tfrac{1}{2}\left[E_i^e(J = 1) - E_i(J = 0) \right] \quad \text{for} \quad i = 0, 1, 3.
\end{aligned}
\tag{14}
$$

The substitution of the atomic masses with the nuclear masses affects the wavenumbers of the ν_1, ν_2, ν_3 vibrations by 0.8, 0.08, and 0.27 cm^{-1}, respectively. The ℓ-type doubling constant $\widetilde{q}_2$ is changed by 0.09 MHz. The rotational constants $\widetilde{B}_0$, $\widetilde{B}_1$, and $\widetilde{B}_3$ are increased by 15 MHz.

To quantify the degree of quasilinearity of molecular vibrations, Yamada and Winnewisser[75] introduced the quasilinearity parameter γ_0. In the nomenclature of linear molecules, γ_0 is defined by

$$
\gamma_0 = 1 - 4\,\frac{E_{0,1^1,0} - E_0}{E_{0,2^0,0} - E_0},
\tag{15}
$$

yielding $\gamma_0 = -1$ for a typical linear molecule and $\gamma = 1$ for a typical bent molecule. Molecules falling between the two limiting cases are commonly called quasilinear. Our results give $\gamma_0 = -1$ for HCO^+, as expected for a degenerate bending mode in well-behaved linear
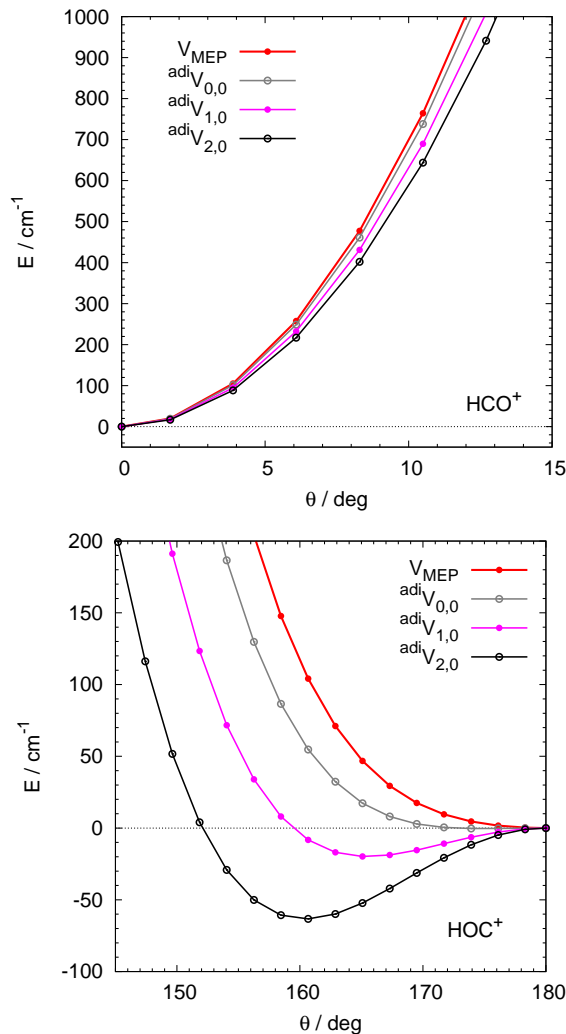
FIG. 1: Minimum energy path V_{MEP} and effective bending potential $^{\mathrm{adi}}V_{v_1,v_3}$ for the $(0,0)$, $(1,0)$ and $(2,0)$ stretching states along the Jacobi angle θ. The curves are shifted to coincide at $\theta = 0°$ for HCO^+ and at $\theta = 180°$ for HOC^+.

To illustrate the internal molecular dynamics in HCO^+ and HOC^+, Figure 1 compares the minimum energy path V_{MEP} along the Jacobi angle θ with the effective bending potentials $^{\mathrm{adi}}V_{v_1,0}$ for the excited ν_1 stretching vibration. The effective bending potentials $^{\mathrm{adi}}V_{v_1,v_3}$ are computed by an adiabatic projection scheme designed for the DVR+DGB approach in the spirit of the method previously developed for tetratomic molecules.[78] The profile $^{\mathrm{adi}}V_{v_1,v_3}$ differs from V_{MEP} by the angle-dependent energy of the stretching state (v_1,v_3), such that $^{\mathrm{adi}}V_{v_1,v_3}$ provides a more useful rationalization of the bending vibration. We see that HCO^+ in Fig. 1 becomes less rigid upon excitation of ν_1, resulting in a lower effective ν_2 bending frequency. For HOC^+, a wide flat region around $180°$ is seen on the minimum energy path and on the effective ground-state profile $^{\mathrm{adi}}V_{0,0}$, where $V_{\mathrm{MEP}}(\theta = 160°)$ and $^{\mathrm{adi}}V_{0,0}(\theta = 160°)$ are approximately 150 and 50 cm^{-1} higher in energy than the corresponding linear arrangements. The excitation of the stretching ν_1 vibration increases the floppyness of HOC^+ since a wider angular region is accessible to ν_2. In addition, HOC^+ becomes effectively bent when the ν_1 vibration is excited. The barrier to linearity is 20 and 60 cm^{-1} for $v_1 = 1$ and $v_1 = 2$, respectively. Bending of a linear molecule upon stretching was previously observed in the case of C_3.[79]

The profiles in Fig. 1 manifest the coupling between the ν_1 and ν_2 vibrational modes. The other effects, such as the radial coupling, the centrifugal distortion effects, or the Coriolis coupling and their influence of the rovibrational structure of HCO^+ and HOC^+ will be addressed in more detail in a future publication.

Our final remark concerns the comparison between experiment and theory. To properly address this issue, in addition to electronic-structure single-point computations, full-dimensional rovibrational calculations in conjunction with a potential energy surface are also required.[80,81] This is especially important in the case of non-rigid and quasilinear molecular systems with strong potential energy couplings between the vibrational modes and strong kinetic-energy (vibration-rotation) couplings.

molecules. For HOC^+, we find $\gamma_0 = -0.75$, such that the two-dimensional bending ν_2 vibration of HOC^+ is a quasilinear mode. For comparison purposes, we note that $\gamma_0 = -0.65$ for the ν_5 vibration of fulminic acid, HCNO,[75,76] and $\gamma_0 = -0.12$ for the ν_5 mode of cyanocarbene, HCCN.[77]

[*] Corresponding author; Electronic address: Mirjana.Mladenovic@u-pem.fr

[1] V. LATTANZI, A. WALTERS, B. J. DROUIN, and J. C. PEARSON, *Astrophys. J.* **662**, 771 (2007).

[2] W. WAGNER-REDEKER, P. R. KEMPER, M. F. JARROLD, and M. T. BOWERS, *J. Chem. Phys.* **83**, 1121 (1985).

[3] M. A. SMITH, S. SCHLEMMER, J. VON RICHTHOFEN, and D. GERLICH, *Astrophys. J. Lett.* **578**, L87 (2002).

[4] S. PETRIE and D. K. BOHME, *Mass Spectrom. Rev.* **26**, 258 (2007).

[5] A. DALGARNO, *Faraday Discuss.* **133**, 9 (2006).

[6] D. BUHL and L. E. SNYDER, *Nature* **228**, 267 (1970).

[7] W. KLEMPERER, *Nature* **127**, 1230 (1970).

[8] R. C. Woods, T. A. Dixon, R. J. Saykally, and P. G. Szanto, *Phys. Rev. Lett.* **35**, 1269 (1975).

[9] M. Bogey, C. Demuynck, and J. Destombes, *Mol. Phys.* **43**, 1043 (1981).

[10] K. V. L. N. Sastry, E. Herbst, and F. C. De Lucia, *J. Chem. Phys.* **75**, 4169 (1981).

[11] R. C. Woods, R. J. Saykally, T. G. Anderson, T. A. Dixon, and P. G. Szanto, *J. Chem. Phys.* **75**, 4256 (1981).

[12] F. Tinti, L. Bizzocchi, C. Degli Esposti, and L. Dore, *Astrophys. J. Lett.* **669**, L113 (2007).

[13] G. Cazzoli, L. Cludi, G. Buffa, and C. Puzzarini, *ApJS* **293**, 1 (2012).

[14] C. S. Gudeman, M. H. Begemann, J. Pfaff, and R. J. Saykally, *Phys. Rev. Lett.* **50**, 727 (1983).

[15] T. Amano, *J. Chem. Phys.* **79**, 3595 (1983).

[16] P. B. Davies and W. J. Rothwell, *J. Chem. Phys.* **81**, 5239 (1984).

[17] K. Kawaguchi, C. Yamada, S. Saito, and E. Hirota, *J. Chem. Phys.* **82**, 1750 (1985).

[18] S. C. Foster, A. R. W. McKellar, and T. J. Sears, *J. Chem. Phys.* **81**, 578 (1984).

[19] P. B. Davies, P. A. Hamilton, , and W. J. Rothwell, *J. Chem. Phys.* **81**, 1598 (1984).

[20] D. J. Liu, S. T. Lee, and T. Oka, *J. Mol. Spectrosc.* **128**, 236 (1988).

[21] C. F. Neese, P. S. Kreynin, and T. Oka, *J. Phys. Chem. A* **117**, 9899 (2013).

[22] C. F. Neese, P. S. Kreynin, and T. Oka, *Journal of Physical Chemistry A* **118**, 5358 (2014).

[23] E. Hirota and Y. Endo, *J. Mol. Spectrosc.* **127**, 527 (1988).

[24] R. J. Foltynowicz, J. D. Robinson, E. J. Zückerman, H. G. Hedderich, and E. R. Grant, *J. Mol. Spectrosc.* **199**, 147 (2000).

[25] R. J. Foltynowicz, J. D. Robinson, and E. R. Grant, *J. Chem. Phys.* **115**, 878 (2001).

[26] J. M. Dyke, N. B. H. Jonathan, A. Morris, and M. J. Winter, *Mol. Phys.* **39**, 629 (1980).

[27] S. M. Vogel, M. C. H. Wright, R. L. Plambeck, and W. J. Welch, *Astrophys. J.* **283**, 655 (1984).

[28] H. J. van Langevelde, E. F. van Dischoeck, and G. A. Blake, *Astrophys. J.* **425**, L45 (1994).

[29] H. S. Liszt and R. Lucas, *Astrophys. J. Lett.* **431**, L131 (1994).

[30] A. E. Glassgold, R. Lucas, and A. Omont, *Astron. Astrophys.* **157**, 35 (1986).

[31] E. F. van Dishoeck, W.-F. Thi, and G.-J. van Zadelhoff, *Astron. Astrophys.* **400**, L1 (2003).

[32] R. Teague, D. Semenov, S. Guilloteau, T. Henning, A. Dutrey, V. Wakelam, E. Chapillon, and V. Pietu, *Astron. Astrophys.* **574**, A137 (2015).

[33] C. S. Gudeman and R. C. Woods, *Phys. Rev. Lett.* **48**, 1344 (1982).

[34] C. S. Gudeman and R. C. Woods, *Phys. Rev. Lett.* **48**, 1768 (1982).

[35] G. A. Blake, P. Helminger, E. Herbst, and F. C. D. Lucia, *Astrophys. J.* **264**, L69 (1983).

[36] R. C. Woods, C. S. Gudeman, R. L. Dickman, P. F. Goldsmith, G. R. Huguenin, W. M. Irvine, A. Hjalmarson, L.-A. Nyman, and H. Olofsson, *Astrophys. J.* **270**, 583 (1983).

[37] L. M. Ziurys and A. J. Apponi, *Astrophys. J. Lett.* **455**, L73 (1995).

[38] A. J. Apponi, T. C. Pesch, and L. M. Ziurys, *Astrophys. J. Lett.* **519**, L89 (1999).

[39] Liszt, H., Lucas, R., and Black, J. H., *Astron. Astrophys.* **428**, 117 (2004).

[40] C. Savage and L. M. Ziurys, *Astrophys. J.* **616**, 966 (2004).

[41] T. Amano, *Philos. Trans. Roy. Soc. A* **324**, 163 (1988).

[42] E. Herbst and D. E. Woon, *Astrophys. J. Lett.* **463**, L113 (1996).

[43] T. Nakanaga and T. Amano, *J. Mol. Spectrosc.* **121**, 502 (1987).

[44] T. Amano, *J. Mol. Spectrosc.* **139**, 457 (1990).

[45] T. Amano and A. Maeda, *J. Mol. Spectrosc.* **203**, 140 (2000).

[46] M. Guelin and P. Thaddeus, *Astrophys. J. Lett.* **227**, L139 (1979).

[47] M. Guelin, J. Cernicharo, and R. A. Linke, *Astrophys. J. Lett.* **263**, L89 (1982).

[48] M. Bogey, C. Demuynck, and J. Destombes, *J. Mol. Spectrosc.* **115**, 229 (1986).

[49] L. Dore, C. Puzzarini, and G. Cazzoli, *Can. J. Phys.* **79**, 359 (2001).

[50] P. Caselli and L. Dore, *Astron. Astrophys.* **433**, 1145 (2005).

[51] NOEMA, http://iram-institute.org/EN/, Accessed: 2017-07-07.

[52] W. D. Watson, V. G. Anicich, and W. T. Huntress, Jr., *Astrophys. J. Lett.* **205**, L165 (1976).

[53] A. Dalgarno and J. H. Black, *Rep. Prog. Phys.* **39**, 573 (1976).

[54] E. D. Young, A. Galy, and H. Nagahara, *Geochimica et Cosmochimica Acta* **66**, 1095 (2002).

[55] M. Mladenović and E. Roueff, *Astron. Astrophys.* **566**, A144 (2014).

[56] M. Mladenović and E. Roueff, *Astron. Astrophys.* (2017).

[57] M. Mladenović and S. Schmatz, *J. Chem. Phys.* **109**, 4456 (1998).

[58] W. H. Press, B. P. Flannery, S. A. Teukolsky, and W. T. Vetterling, *Numerical Recipes, Example Book (Fortran)*, Cambridge University Press, Cambridge, 1985.

[59] I. Mills, T. Cvitaš, K. Homann, N. Kallay, and K. Kuchitsu, *Quantities, Units and Symbols in Physical Chemistry, Second Edition*, Blackwell Scientific Publications, Oxford, 1993.

[60] M. Mladenović, *J. Chem. Phys.* **112**, 1070 (2000).

[61] M. Mladenović and Z. Bačić, *J. Chem. Phys.* **93**, 3039 (1990).

[62] C. Puzzarini, R. Tarroni, P. Palmieri, S. Carter, and L. Dore, *Mol. Phys.* **87**, 879 (1996).

[63] T. Hirao, S. Yu, and T. Amano, *J. Mol. Spectrosc.* **248**, 26 (2008).

[64] R. J. Foltynowicz, J. D. Robinson, and E. R. Grant, *J. Chem. Phys.* **114**, 5224 (2001).

[65] T. Hirao, S. Yu, and T. Amano, *J. Chem. Phys.* **127**, 074301 (2007).

[66] J. M. Brown, J. T. Hougen, K. P. Huber, J. W. C. Johns, L. Kopp, H. Lefebvre-Brion, A. J. Merer, D. A. Ramsay, J. Rostas, and R. N. Zare, *J. Mol. Spectrosc.* **55**, 500 (1975).

[67] G. Herzberg, *Molecular Spectra & Molecular Structure Vol. II, Infrared and Raman Spectra of Polyatomic Molecules (corrected reprint of 1945 edition)*, Krieger, Malabar FL, 1991.

[68] P. Botschwina, S. Seeger, M. Horn, J. Flügge, M. Oswald, M. Mladenović, U. Höper, R. Oswald, and E. Schick, Quantum-chemical calculations on molecules of astrochemical interest, in *Molecules and Grains in Space*, edited by I. Nenner, AIP Conference Proceedings 312, pp. 321–336, Woodbury, NY, 1994, AIP.

[69] L. Dore, S. Beninati, C. Puzzarini, and G. Cazzoli, *J. Chem. Phys.* **118**, 7857 (2003).

[70] G. Czakó, E. Mátyus, A. C. Simmonett, A. G. Császár, H. F. Schaefer III, and W. D. Allen, *J. Chem. Theory Comput.* **4**, 1220 (2008).

[71] J. M. L. Martin, P. R. Taylor, and T. J. Lee, *J. Chem. Phys.* **99**, 286 (1993).

[72] P. Henning, W. P. Kraemer, and G. H. F. Diercksen, *A compilation of theoretical spectroscopic constants and rotational-vibrational transition frequencies for the isoelectronic series of linear triatomic molecules HCN, HNC, HCO^+, HOC^+, HNN^+ obtained from ab initio calculated energy hypersurfaces*, Internal Report, MPI/PAE Astro 135, Max-Planck Institut, München, 1977.

[73] W. Kraemer and P. Bunker, *J. Mol. Spectrosc.* **101**, 379 (1983).

[74] Note a misprint in Table X of Ref. 69, where $B_e(\text{HC}^{18}\text{O}^+)$ should have a value of $42\,811.0181(16)$ MHz.

[75] K. Yamada and M. Winnewisser, *Z. Naturforsch. A* **31**, 139 (1976).

[76] M. Mladenović, M. Elhiyani, and M. Lewerenz, *J. Chem. Phys.* **130**, 154109 (2009).

[77] M. Mladenović, P. Botschwina, and C. Puzzarini, *J. Phys. Chem. A* **110**, 5520 (2006).

[78] M. Mladenović, *Spectrochim. Acta, Part A* **58**, 795 (2002).

[79] M. Mladenović, S. Schmatz, and P. Botschwina, *J. Chem. Phys.* **101**, 5891 (1994).

[80] M. Mladenović, *J. Chem. Phys.* **137**, 014306 (2012).

[81] M. Mladenović, *J. Chem. Phys.* **141**, 224304 (2014).